

## Supplementary Information

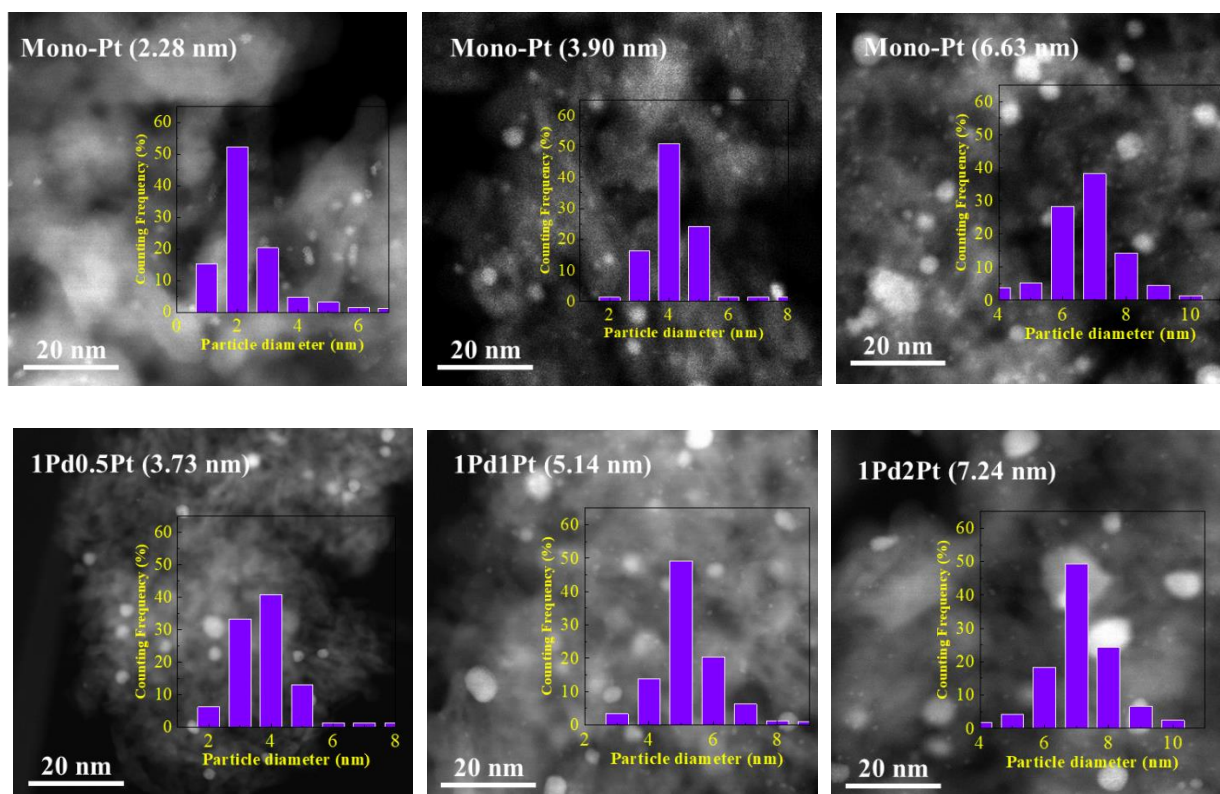
The normalization of active surface site of bimetallic Pd-Pt catalyst, their inhomogeneity, and their roles in methane activation

Haojie Geng<sup>1,\*</sup>, Zhongqing Yang<sup>2</sup>, Haobo Zhao<sup>1</sup>, Siyu Yu<sup>1</sup>, Hong Lei<sup>1</sup>

1. School of Chemistry and Chemical Engineering, Southwest University, Chongqing 400715, China
2. School of Energy and Power Engineering, Chongqing University, Chongqing 400030, China

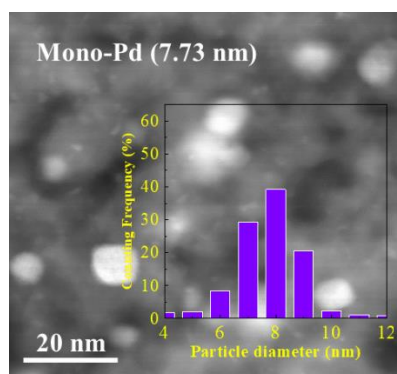
### S1 Particle size distribution of Pd-Pt nanoparticles

Particle size distributions of Pd-Pt samples are characterized by TEM method, shown in **Figure S1**. These samples possess different diameter distributions.



Corresponding author:

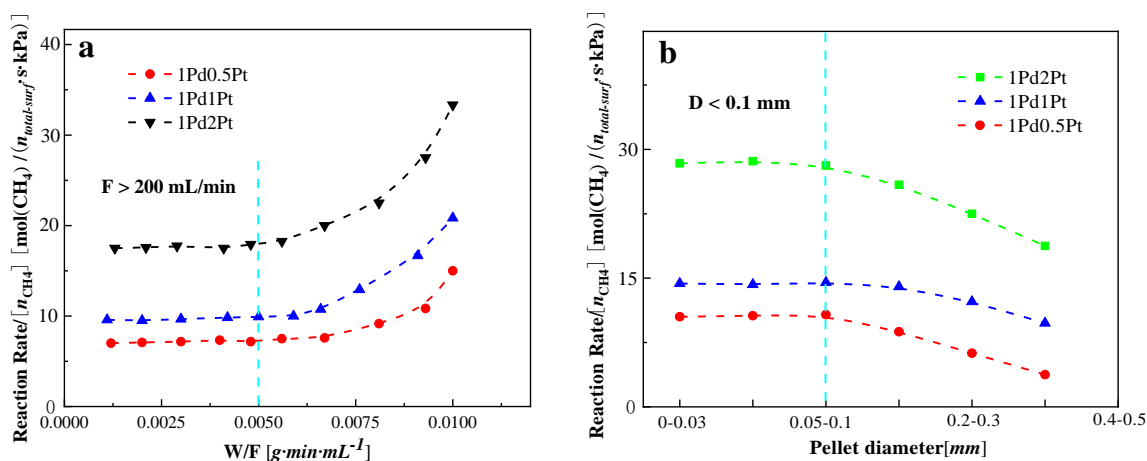
\* Name: Haojie Geng, Ph.D, Lecturer, Email: hjgeng@swu.edu.cn;



**Figure S1.** Particle size distribution of Pd-Pt nanoparticles characterized by TEM method

### S2 External and internal diffusion for catalytic reaction

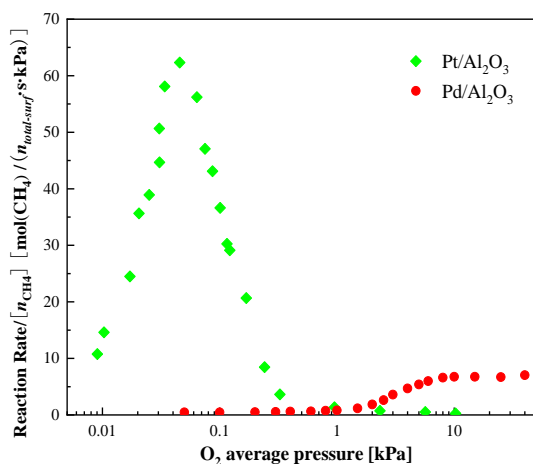
To eliminate the influence of external and internal diffusion of catalytic reactions, we performed the diffusion experiment, see **Figure S2**. When the total flow rate was higher than 200 mL/min, external diffusion was eliminated and reaction rates did not vary with changing WHSV. And the diameters of catalyst pellets should be lower than 0.1 mm, to eliminate the internal diffusion for catalytic reaction.



**Figure S2.** Inspection and elimination of external and internal diffusion for catalytic reaction (**a**, external diffusion; **b**, internal diffusion; “**W**” stands for catalyst mass loading (1 g) and “**F**” stands for total flow rate (mL/min))

### S3 Catalytic performance of Pd and Pt species

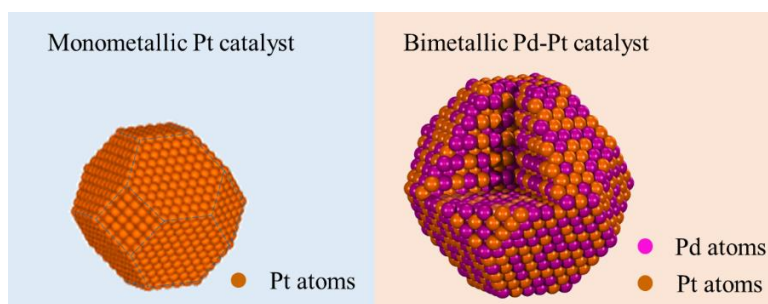
**Figure S3** displays methane catalytic reaction rates over monometallic Pd (7.73 nm) and Pt (6.68 nm) catalysts at 300 °C. Methane pressure was set at 0.5 kPa, and oxygen pressure varied in a wide range from 0.001 kPa to 50 kPa. As the oxygen pressure was varied, we found that the Pd and Pt species showed different catalytic performances in the reaction. Pt species are highly active at low oxygen pressures, whereas Pd species show high catalytic performances under oxygen-rich conditions.



**Figure S3.** Methane catalytic reaction rate over monometallic Pd (7.73 nm) and Pt (6.68 nm) catalyst (0.5 kPa CH<sub>4</sub>, N<sub>2</sub> balance, 300°C)

#### S4 Particle model

**Figure S4** shows the cubo-octahedron model for monometallic Pt and bimetallic Pd-Pt catalysts. The crystals formed by Pd or Pt element have face-centered cubic structure. Atomic radius of Pd is 1.79 Å, and Pt is 1.83 Å. For bimetallic Pd-Pt catalysts, Pd and Pt were randomly distributed on the particle surface.



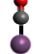








**Figure S4.** Catalyst particle model for monometallic Pt and bimetallic Pd-Pt catalysts

#### S5 Assignments of infrared absorption bands

**Table S1** displays the assignments of infrared absorption bands used for deconvolution of Pd-Pt catalysts. In this experiment, CO molecules flowed through catalyst bed and adsorbed on surface active sites. MCT detector received infrared signal of catalyst surface species, and vibration signal of C-O bond was selected to identify the type of surface active sites [1, 2]. Via CO uptake, wavenumber of infrared spectrum of C-O bond vibration located in the range of 1700 cm<sup>-1</sup> to 2300 cm<sup>-1</sup> [3, 4]. To depict the structure of CO adsorption in detail, we performed spectral deconvolution over “Peak-Fitting” software via methodology of “Deconvolution-AutoFit”. The spectral deconvolution was adjusted according to the following information in **Table S1**. Peak center location and full widths at half height (FWHM) were limited in a small variation range with error of ±2 cm<sup>-1</sup> wavenumber. So we mainly adjusted the height parameter to do spectral deconvolution. The determination coefficient (R<sup>2</sup>) was higher than 0.98, which was used to evaluate the reasonability of fitting outcomes statistically.

**Table S1.** Assignments of infrared absorption bands used for deconvolution of Pd-Pt catalysts [5-12]

| Structure   | Assignment  | Wavenumber [cm <sup>-1</sup> ] | FWHH [cm <sup>-1</sup> ] |
|---|---|--------------------------------|--------------------------|
| <b>IR peak assignments for Pd species</b>   |   |                                |                          |
|    | CO three-fold adsorption on Pd <sup>0</sup>                                 | 1890                           | 115                      |
|    | CO bridged adsorption on Pd <sup>0</sup> terraces and edges, respectively   | 1940, 1985                     | 58, 27                   |
|    | CO linear adsorption on Pd <sup>0</sup> edges and terraces, respectively    | 2060, 2080                     | 25, 21                   |
|    | CO bridged adsorption on Pd <sup>+</sup>                                    | 1970                           | 54                       |
|    | CO linear adsorption on Pd <sup>+</sup> and Pd <sup>2+</sup> , respectively | 2105, 2145                     | 25, 96                   |
| <b>IR peak assignments for Pt species</b>   |   |                                |                          |
|    | CO bridged adsorption on Pt <sup>0</sup>                                    | 1820                           | 80                       |
|    | CO linear adsorption on Pt <sup>0</sup> corners and edges                   | 2040, 2065, 2085               | 55, 25, 35               |
|  | CO adsorption on Pt <sup>0</sup> terraces                                   | 2097                           | 6                        |
|  | CO adsorption on Pt <sup>δ+</sup>   | 2115                           | 32                       |

Note: The error of wavenumber is  $\pm 2$  cm<sup>-1</sup>.

## Reference

- [1] Z. Liu, A. Rittermeier, M. Becker, K. Kähler, E. Löffler, M. Muhler, High-pressure CO adsorption on Cu-based catalysts: Zn-induced formation of strongly bound CO monitored by ATR-IR spectroscopy, *Langmuir*, 27 (2011) 4728-4733.
- [2] A. Sumer, A.E. Aksoylu, Adsorption-induced surface electronic reconstruction of Pt and Pt-Sn alloys during CO adsorption, *The Journal of Physical Chemistry C*, 113 (2009) 14329-14334.
- [3] G.T.K.K. Gunasooriya, M. Saeys, CO adsorption on Pt(111): From isolated molecules to ordered high-coverage structures, *ACS Catalysis*, 8 (2018) 10225-10233.
- [4] I.V. Yudanov, R. Sahnoun, K.M. Neyman, N. Rösch, J. Hoffmann, S. Schauer mann, V. Johánek, H. Unterhalt, G. Rupprechter, J. Libuda, H.-J. Freund, CO adsorption on Pd nanoparticles: Density functional and vibrational spectroscopy studies, *The Journal of Physical Chemistry B*, 107 (2003) 255-264.
- [5] M.J. Kale, P. Christopher, Utilizing quantitative in situ FTIR spectroscopy to identify well-coordinated Pt atoms as the active site for CO oxidation on Al<sub>2</sub>O<sub>3</sub>-supported Pt catalysts, *Acs Catalysis*, 6 (2016) 5599-5609.
- [6] R.K. Brandt, R.S. Sorbello, R.G. Greenler, Site-specific, coupled-harmonic-oscillator model of carbon-monoxide adsorbed on extended, single-crystal surfaces and on small crystals of platinum, *Surface Science*, 271 (1992) 605-615.
- [7] K. Ding, A. Gulec, A.M. Johnson, N.M. Schweitzer, G.D. Stucky, L.D. Marks, P.C. Stair, Identification of active sites in CO oxidation and water-gas shift over supported Pt catalysts, *Science*, 350 (2015) 189-192.

- [8] R. Barth, R. Pitchai, R.L. Anderson, X.E. Verykios, Thermal desorption-infrared study of carbon monoxide adsorption by alumina-supported platinum, *Journal of Catalysis*, 116 (1989) 61-70.
- [9] W.G. Rothschild, H.C. Yao, H.K. Plummer, Surface interaction in the platinum- $\gamma$ -alumina system. V. Effects of atmosphere and fractal topology on the sintering of platinum, *Langmuir*, 2 (1986) 588-593.
- [10] J. Szanyi, J.H. Kwak, Dissecting the steps of CO<sub>2</sub> reduction: 2. The interaction of CO and CO<sub>2</sub> with Pd/ $\gamma$ -Al<sub>2</sub>O<sub>3</sub>: an in situ FTIR study, *Physical Chemistry Chemical Physics*, 16 (2014) 15126-15138.
- [11] M. Moses-DeBusk, M. Yoon, L.F. Allard, D.R. Mullins, Z. Wu, X. Yang, G. Veith, G.M. Stocks, C.K. Narula, CO oxidation on supported single Pt atoms: Experimental and ab initio density functional studies of CO interaction with Pt atom on  $\theta$ -Al<sub>2</sub>O<sub>3</sub>(010) surface, *Journal of the American Chemical Society*, 135 (2013) 12634-12645.
- [12] L.-C. de M nerval, A. Chaqroune, B. Coq, F. Figueras, Characterization of mono- and bi-metallic platinum catalysts using CO FTIR spectroscopy Size effects and topological segregation, *Journal of the Chemical Society, Faraday Transactions*, 93 (1997) 3715-3720.